Phase-Field Modelling of Stress Corrosion

Per Ståhle [1,a] and Eskil Hansen [2,b]

[1] Div. of Solid Mechanics, Lund University, Lund Sweden

[2] Centre for Mathematical Sciences, Lund University, Lund Sweden

[a] per.stahle@solid.lth.se, [b] eskil.hansen@appl.math.lth.se

Keywords: Stress corrosion, crack initiation, surface morphology, pitting, phase field model, anti-plane strain.

Abstract. The evolution of surfaces exposed to an aggressive environment and mechanical load is studied. The evolution is the initial part of a stress corrosion process that leads to pitting, crack initiation and growing cracks. In conventional fracture analyses the growth rate of the crack may be computed using a modified Paris' law. However, a known or a postulated crack is required. A serious drawback is that a large part of the lifetime of a crack or a surface flaw is spent during the initiation of the crack. The knowledge of the mechanisms leading from a pit, flaw, scratch, etc. to a crack is very limited. One reason is the complication caused by the less definite defined original geometry. The motivation for the present study is to increase the understanding of the transition from stress induced pitting to growing cracks.

Introduction

A strained body exposed to an aggressive environment may suffer from continuous material dissolution during corrosion. The result is a progressive roughening of its surfaces. After roughening pitting occurs and eventually cracks will form and grow into the body. Apart from an aggressive environment and a mechanical stress the material needs to have an inherent sensitivity or to be sensitized to the environment. This can be due to local heating, plastic deformation, fatigue damage, etc. The aggressive environment can be a bulk aqueous environment surrounding the body or a micro environment, such as moist in pits, crevices, under deposits and not seldom very local environments created by microbial colonies established on the body surface.

The corrosion process produces a thin film of metal oxides or hydroxides or compounds thereof. Even though the thickness of this film is typically not more than a few nanometres, it reduces the rate of dissolution by several orders of magnitude. If kept intact, this protective film would increase the service life of an exposed structure tremendously. However, occasionally or repeatedly the film is damaged as a result of variation in load, electro-chemical environment or, as was recently discovered, by microbiological activity. Some microbes may even have the oxide film or the substrate as an essential component of their metabolism (cf. ASME [1]; Beech and Sunner [2]).

The focus here is on the evolving surface morphology and initiation of cracks caused by the corrosion. The mechanism is the mass transportation resulting after dissolution and diffusion of matter into the environment or surface diffusion (see Fig. 1). The strain energy and the chemical energy provide driving forces for dissolution and transport of molecules. The observation is an evolving surface waviness that has been explained theoretically by [3-5]. The spectrum of the waves depends on the strain energy of the body surface and the surface energy. The elastic strain energy tends to increase the waviness of the surface whereas the surface energy tends to decrease the waviness. Waves with wavelengths longer than a stress dependent critical wavelength grow, while waves with shorter wavelengths decay. Experimental results by Kim et al. [5] show that the typical wavelength in, e.g., aluminium is on the scale of a few hundred nanometres when the stress is large and comparable to the yield stress.

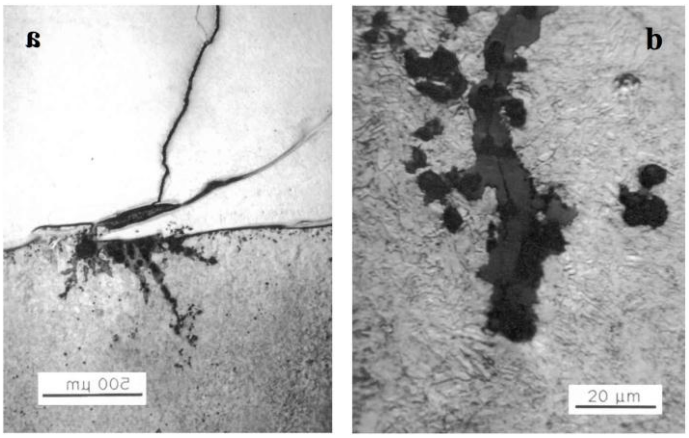

Fig.1. a) Corrosion crack penetrating a bimaterial interface between austenitic steel and pressure vessel steel of type SA533C11. b) The tip of one of the crack branches. Note that the widest part of the crack is at the crack tip. Crack length is 7 mm and notch width is around 10 μm. Reproduced with permission from Vattenfall AB, Sweden.

Several non-linear analyses show that the indents grow markedly faster and the peaks of the surface grow slower. This sharpens the indents and leads to a formation of pits. The prediction is that the indents eventually approach a singular state, where the deepest part of the indents locally assumes the geometry of a sharp crack tip or a cusp. In earlier studies [6,7], the dissolution was assumed to be a function only of the stretching of the surface. A threshold strain was invoked to comply with the limited elastic properties of the oxide film. It was then predicted that the indent sharpens and become crack like. Thereafter, growth continues in the form of a blunted crack or, in a strict sense a deep notch with a relatively sharp tip. Fig. 1 b) shows a real stress corrosion crack in a nuclear pressure vessel. The crack tip always preserves a finite radius that may depend on the crack tip driving force and the thermodynamic chemical and mechanical properties of the surface. Further, the crack frequently branches and the crack width becomes slightly larger as the crack gets longer.

Phase field modelling

For a virtually sharp surface, treated as a discontinuity, specific chemical and mechanical properties may be ascribed to the surface. This simplifies the analysis and has normally no significant influence on the thermodynamical behaviour of the body. However, when the distance between structural inhomogeneities or other characteristic distances are of the same order of magnitude as the thickness of the surface, e.g., as at a rough surface, at the tip of a crack or during emission of dislocations etc., the thickness of the surface may play a role and the negligence thereof may lead to unrealistic predictions. As opposed to this, a diffuse surface model assumes a continuous variation of composition, structure and other properties within the modelled region (cf. Landau and Lifshitz [8]). This includes the body, the diffuse surface and the surrounding environment. Here, the total free energy of the continuous body is formulated as a function of the material composition. The width of the surface layer is not assumed given, but instead the model predicts surface layers with a finite width and the associated surface energy is a result of the thermodynamical state of the material composition of the surface. A diffuse interface model was first applied by Cahn and Hilliard [9], to study the thermodynamics of a coherent interface between two phases. Their predictions include the width of the interface and the corresponding interfacial energy.

Phase fields. For a general case two types of so-called order parameters are introduced to model the compositional and structural non-uniformities. An order parameter is defined as a continuous field that is referred to as a phase field. The total free energy of the system is formulated as a function of the phase fields. The variation of the free energy with respect to the fields act as driving forces for the evolution over time, following the Cahn-Hilliard equation for the conserved order parameters

and the Ginzburg-Landau equation for the non-conserved order parameters. In the proposed study an order parameter, ψ, is used to distinguish empty space from the solid and to model the properties of the surface of the body.

The goal of this paper is to use relevant physical properties of the surface layer so that the evolution of the corroding body can be captured. The modelling results in the formation of pits, initiation and growth of cracks and crack branching despite that no criteria is applied for any of the mentioned events. The tendency to instable surface behaviour is inherent in the model and thus no criteria are needed. The body is assumed to be isotropic with a surface energy defined for a planar surface in the selected environment. Further, the body is assumed to remain in mechanical equilibrium. The tendency of the surface to change the shape of its reference configuration is governed by a chemical potential. As the surface configuration is varied, the positive surface energy tends to flatten the surface while the positive strain energy is inclined to roughen the surface.

The fundamental problem is for a semi-infinte body with a planar surface representing the initial structure. A Cartesian coordinate system x_1, x_2 and x_3 is giving a two dimensional representation of the body, in the plane $x_3 = 0$. The initial plane surface coincide with $x_2 = 0$, dividing the space into the half plane, $x_2 \leq 0$, initially covered by the body and the halfplane, $x_2 > 0$, that is empty. In its initial configuration, the surface region, i.e. the transition region between the empty space and the solid body, is small compared to the linear extent of the considered geometry. The evolution of the body is obtained by minimizing the free energy. This is achieved by formulating the total energy as a functional of the phase field. From this the kinetics is derived along the steepest descent path of the total energy, using the time-dependent Ginzburg–Landau equation. In the present study the total energy of the structure consists of an elastic strain energy, a chemical energy and a gradient energy. The variations of these energies are assumed to be the only driving forces evolving the surface morphology.

The solid material is assumed to be linear elastic with the elastic modulus E_o and Poisson's ratio v. The total energy of the system is composed of the Landau chemical potential energy, F_{ch}, the gradient energy, F_{gr}, and the elastic energy, F_{el} as follows:

$$F = F_{ch} + F_{gr} + F_{el} \,. \tag{1}$$

Here the Landau chemical potential energy is defined by

$$F_{ch} = U(\psi). \tag{2}$$

For a thermo dynamical treatment of phase transformation $U(\psi)$ is obtained from a phase diagram. The compositional parameter ψ is defined in the interval $|\psi| \leq 1$, where $\psi = 1$ denotes the body and $\Phi = -1$ denotes empty space. Therefore a double-well Landau potential with the requirements that $U'(\pm 1) = 0$ and $U''(\pm 1) = 0$ is selected. The simplest polynominal would be the symmetric double-well potential

$$U(\psi) = p\left(\frac{1}{4}\psi^4 - \frac{1}{2}\psi^2\right). \tag{3}$$

The gradient energy is given as follows

$$F_{gr} = \frac{g_b}{2}(\nabla\psi)^2. \tag{4}$$

The material parameter, g_b, is related to the thickness of the surface.

The body has the elastic modulus E_o and a Poisson's ratio ν. The elastic modulus is a function of the composition, i.e., $E = E(\psi)$ in the entire modelled region. It should approach the elastic modulus of the solid, E_o, as $\psi \to 1$ and vanish as $\psi \to -1$ and the thermodynamic driving force should vanish as $|\psi| \to 1$ which leads to the requirement $E'(\psi) \to 0$ as $|\psi| \to 1$. The simplest polynominal approach that fulfil the requirements is

$$E(\psi) = -\frac{1}{4}(\psi^3 - 3\psi - 2)E_o, \tag{5}$$

Poisson's ratio ν is assumed to be independent of ψ. The elastic deformation of the virtually empty space occurs at insignificant stress. To simplify the analysis anti-plane deformation is assumed. Thus, the only remaining displacement component is u_3 and the elastic strain energy is given by

$$F_{el} = \frac{E(\psi)}{4(1+\nu)}(\nabla u_3)^2. \tag{6}$$

The Ginzburg-Landau equation, applicable for non-conserved quantities is used for matter in this case. This is because the corrosion is assumed to be a consuming process at which matter disappear. Thus, the evolution of the composition parameter, ψ is given as the rate $\partial\psi/\partial t$ proportional to the variation of the free energy, as follows:

$$\frac{\partial\psi}{\partial t} = -L_\psi \frac{\delta F}{\delta\psi}, \tag{7}$$

where L_ψ is a mobility parameter (cf. Cahn and Hilliard [9]). According to Lagranian formalism the variation is given by,

$$\frac{\delta F}{\delta\psi} = \frac{\partial F}{\partial\psi} - \nabla\cdot\frac{\partial F}{\partial(\nabla\psi)}. \tag{8}$$

For the order parameter ψ and application of (7), insertion of (3), (2) and (4) into (8) gives the governing equation for the evolution of ψ,

$$\frac{\partial\psi}{\partial t} = -L_\psi\{[\frac{3E_o}{16(1+\nu)}(\nabla u_3)^2 + p\psi](\psi^2 - 1) - g_b\nabla^2\psi\}. \tag{9}$$

Applying (8) for the displacements gives the following governing equation,

$$\frac{\partial u_3}{\partial t} = -L_u\{\nabla^2 u_3 + \frac{3(\psi-1)}{4(\psi+1)(\psi-2)}(\nabla\psi\nabla)u_3\}. \tag{10}$$

The equations (9) and (10) are solved for different initial conditions for ψ and boundary conditions for ψ and u. The initial conditions of ψ define the initial shape of the body. For the integration of (9), the mobility constant L_u is chosen sufficient large, so that close to static conditions are achieved. The desired goal is to fulfil mechanical equilibrium, i.e. $\partial u_3/\partial t$.

The resulting equations (9) and (10) constitute a system of nonlinear elliptic-parabolic equations. Solutions for given initial conditions and boundary conditions is obtained by combining splitting methods with a semi-implicit time stepping scheme using finite differences. The calculations are performed in a moving coordinate system where the known solution for a straight corroding edge is subtracted from the sought solution.

The model

Consider a large body with a traction free wavy edge, with a wave amplitude ω and the wavelength λ (see Fig. 2). The body initially occupies the region $x_1 < \omega\sin(x_2 2\pi/\lambda)$ and the rest is defined as

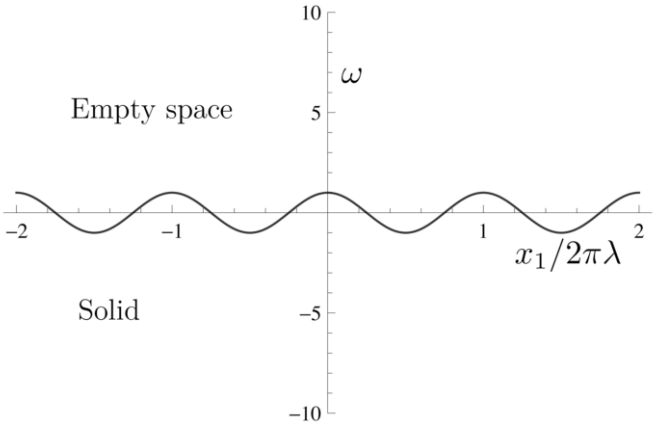

Fig. 2. Wavy initial body surface with wavelength λ and wave amplitude ω.

empty space. Strictly, this would imply that $\psi = 1$ in the region covered by the body and $\psi = -1$ in the remaining body. However, this would not meet the requirement $|\psi| < 1$. To avoid this inconsistency, the initial field ψ is chosen to be

$$\psi = -\tanh\left(\frac{x_1 + \omega \sin(x_2 2\pi / \lambda)}{\varepsilon}\right), \tag{11}$$

where the parameter ε determines the thickness of the layer where ψ shifts from near 1 to near -1. A remote shear $\partial\psi / \partial x_1$ is prescribed as $\sqrt{x_1^2 + x_2^2} \to \infty$.

$$\frac{\partial\psi}{\partial x_1} = 0 \quad \text{and} \quad u_3 = \lambda\gamma \quad \text{at} \quad |x_1| = \frac{\lambda}{2}, \tag{12}$$

$$\psi \to 1 \quad \text{and} \quad \sigma_{23} \to 0 \quad \text{as} \quad x_2 \to -\infty, \tag{13}$$

$$\text{and} \quad \psi \to -1 \quad \text{and} \quad \sigma_{23} \to 0 \quad \text{as} \quad x_2 \to \infty, \tag{14}$$

As a result of the analysis as the shear modulus vanishes in the space outside the body this will ensure that the body surface becomes traction free.

Results and discussion

First the problem for a straight edge is studied, i.e. $\omega/\lambda = 0$ without mechanical load. The resulting phase field ψ is shown in Fig. 3. The result from two different mesh sizes may be compared. For the courser mesh the resolution is around 5 nodal points covering boundary layer within which the phase undergo the transition from solid body to virtually empty space. With the finer mesh, the boundary width is covered by around 10 mesh elements. The markers indicate the mesh resolution. Included in the figure is the analytical result by Ginzburg and Landau [10],

$$\psi = -\tanh\sqrt{\frac{p}{2g_b}}x_2 . \tag{15}$$

As observed the finer resolution gives very accurate results. The width of the boundary region is around 6 to 8 times $\sqrt{2g_b / p}$. About 10 elements seem to be sufficient to achieve a good accuracy. This resolution is selected for the remaining study.

An applied stress results in a dissolution of material at the edge of the body, e.g. the propagation rate of the edge, e.g. the contour $\psi = 0$, is

$$c = 3L_\psi\{E_o\gamma^2 / 2(1+\nu)\}\sqrt{g_b / 2p}\,. \tag{16}$$

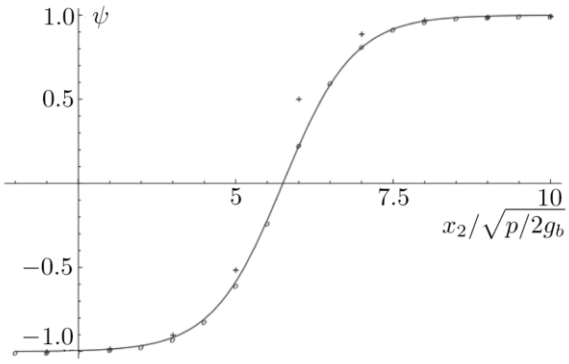

Fig. 3. The phase ψ across the boundary layer region. Analytical solution [10] and numerical with course (+) and fine (o) resolutions. Mechanical load is not applied.

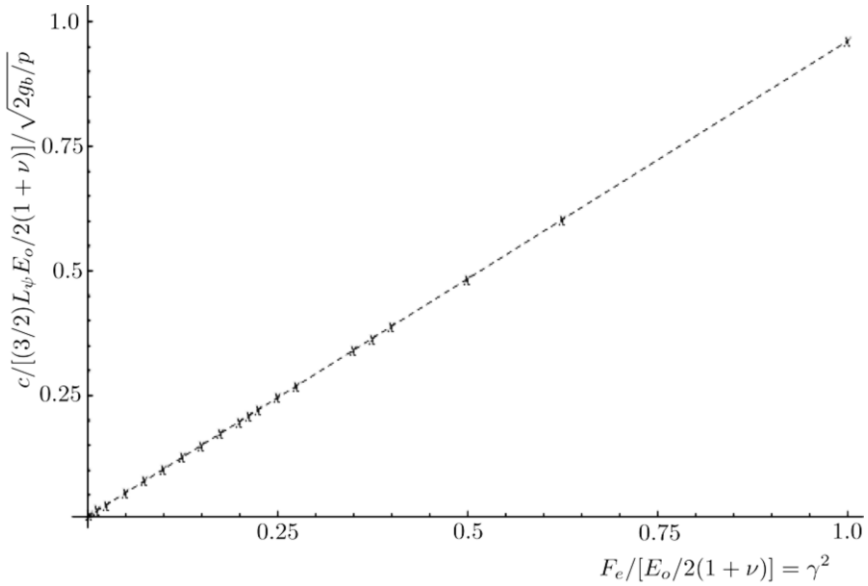

Fig. 4. Dissolution rate as a function of the strain energy density. The dashed line shows the analytical result (16) for the propagation rate of the contour $\psi = 0$. The markers show the numerical result.

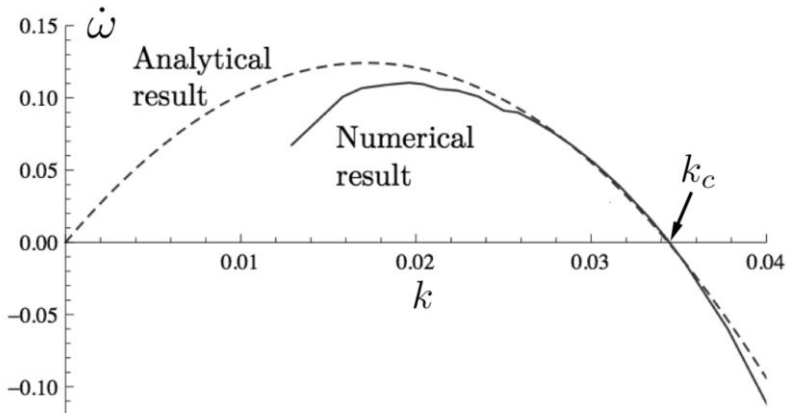

Fig. 5. The growth rate of the amplitude ω of the surface waves as a function of their spatial frequency $k = 2\pi/\lambda$. The dashed curve is the growth rate $\dot{\omega} = \alpha L_\psi E_o (2g_b / p)(k_c - k)k$, where α is a non-dimensional constant.

As observed the dissolution rate is proportional to the strain energy of the material. In Fig. 4 the numerical result is plotted versus strain energy density. As observed the numerical result follow closely the analytical prediction. The result is expected for $\omega/\lambda = 0$. For a wavy surface this linear relation ship between dissolution rate and strain energy is only expected as long as $\omega << \lambda$.

The waviness for $\omega/\lambda \neq 0$ will give different dissolution rates because of the variation of stress that is caused by the non-homogeneous boundary. The dependence of the wave number $k = 2\pi/\lambda$ is shown in Fig. 5. Waves with an over critical wave number decay whereas waves with lower wave number increase in amplitude (see e.g. [6], [5]). The phase field model also features the same behaviour. As the figure shows above the critical wave number, k_c, the growth rate of the wave amplitudes become negative. The agreement with the analytical result for a sharp boundary is reasonable for wave numbers in the vicinity of k_c. For longer waves, $k < 0.5k_c$, the divergence is large and wave numbers less than $0.3k_c$ could not be accurately computed seemingly because of insufficient mesh properties.

Figures 6 a and b show the phase field and the corresponding stress distribution after continued dissolution. As the figure shows, the surface waves develop into pits and cracks the continue to grow in parallel as opposed to the normally observed that one pit or crack take the lead and cause the other to stop because of an insufficient driving force.

In the analysis so called general corrosion of material has been ignored. This refers to the dissolution of material that occur irrespective of mechanical load. To add this effect a phase gradient term is added to according to the following

$$\frac{\partial \psi_g}{\partial t} = \frac{\partial \psi}{\partial t} - \beta L_\psi (\nabla \psi)^2 (2g_b / p) \,, \qquad (17)$$

where β is an arbitrary dimensionless constant. To explore the effect of general corrosion (17) was computed for an initially slightly wavy surface. The result displayed in Fig. 7 compare the result for $\beta = 0$ and $\beta = \{\gamma^2 E_o / 4(1+\nu)\}$, where the latter give a contribution to the dissolution rate comparable to the dissolution caused by the strain energy.

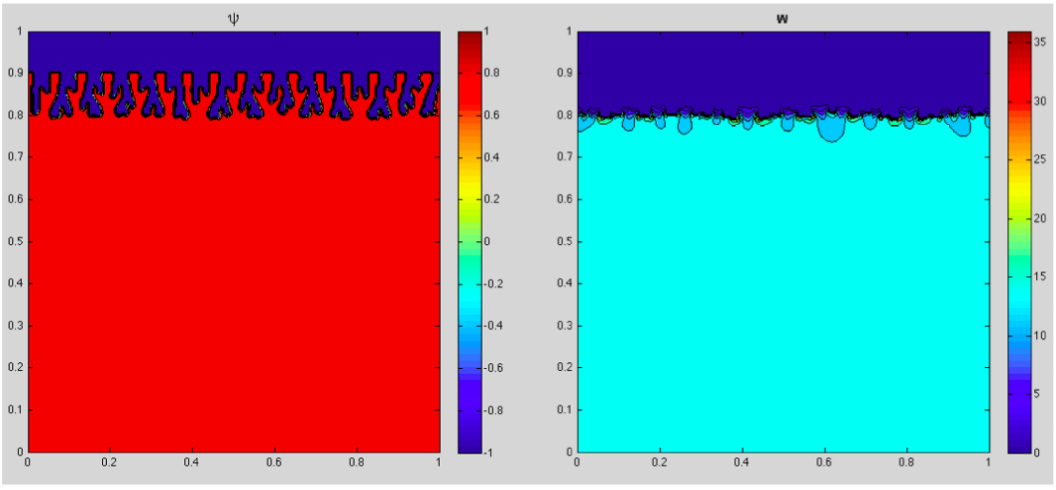

a) b)

Fig. 6. a) The morphology of the unstable surface after the time $t = 1/k_c c_o$. Red shows the solid material and blue is empty space. b) The corresponding distribution of von Mises effective stress $(1+\nu)\sigma_e/\gamma E_o$. At the bottom of the deep notches the stresses are observed to be around 3 times larger than the nominal stress.

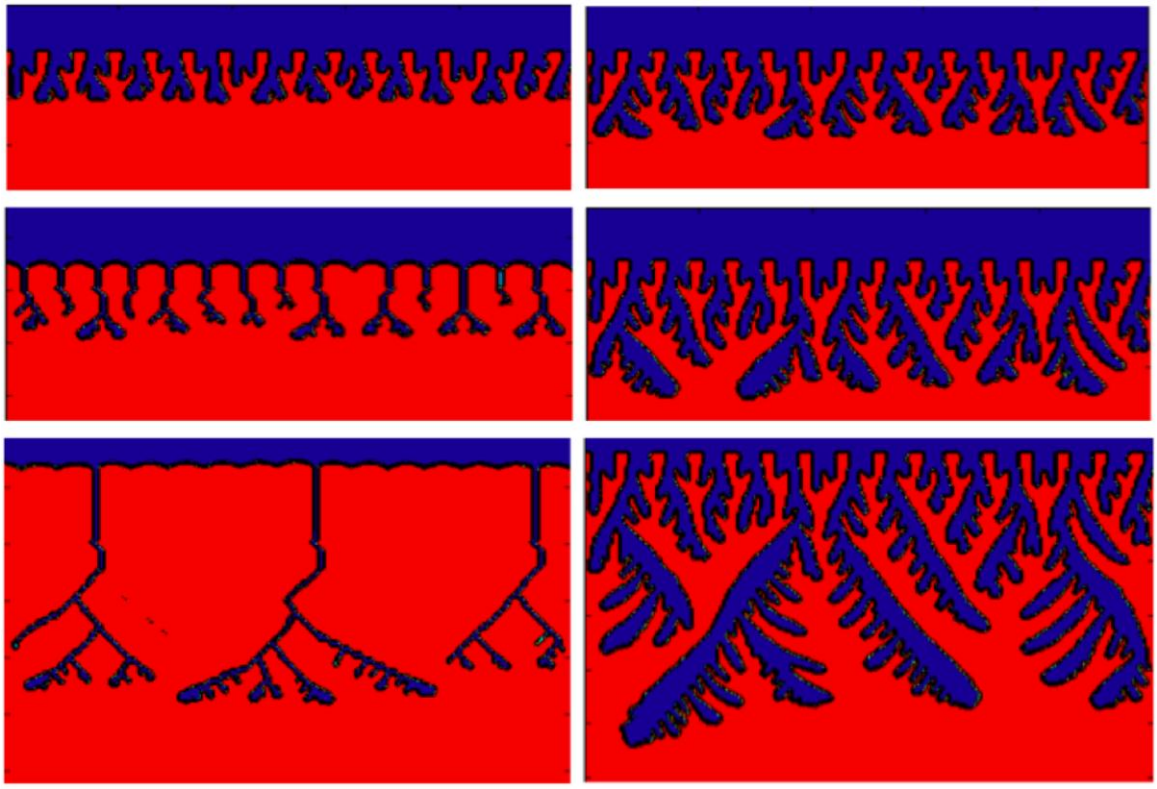

a) b)

Fig. 7. Simulation of stress driven dissolution. Time is increasing from top to bottom. In a) simulation pure stress corrosion and in b) general corrosion is added.

Conclusions

Stress corrosion can be modelled as a moving boundary problem. Phase field modelling simplifies the analysis and the tracking of the moving boundary. The instability of a flat surface subjected to mechanical load is in agreement with results from traditional analyses. Formation cracks and crack growth are captured.

Acknowledgements Support from The Swedish Research Council under grant no 2011-5561 is acknowledged.

References

[1] ASME, American Society of Mechanical Engineers. Materials Handbook, Corrosion, vol. 13. Academic Press (2005)
[2] Beech, I.B., Sunner, J., Curr. Opinion Biotechnol. 15, 181–186 (2004)
[3] Asaro, R.J. and Tiller, W.A., Metall. Trans. 3, 1789 (1972)
[4] Grinfeld, M.A., Sov. Phys. Dokl. 31, 831, 1986; J. Nonlinear Sci. 3, 35 (1993)
[5] Kim, K.S. Hurtado, JA., and Tan, H., Physical Rev. Letters, 83/19 (1999)
[6] Ståhle, P., Bjerken, C., and Jivkov, AP., Int. J. Solids and Struct., 44: p. 1880-1890 (2007)
[7] Jivkov, AP. and Ståhle, P., A Pilote etc. (2004)
[8] Landau L, Lifshitz E. Phys Zeit Sowjetunion 8:153 (1935)
[9] Cahn, J.W., Hilliard J.E., J Chem Phys, 28:258 (1958)
[10] Ginzburg, VL. and Landau, LD., Zh. Eksp. Teor. Fiz. 20, 1064 (1950)